

# Reduction of circuit depth by mapping qubit-based quantum gates to a qudit basis

Pamela Rambow<sup>1</sup> and Mingzhen Tian<sup>2</sup>

Department of Physics and Astronomy, Quantum Science and Engineering Center  
George Mason University, Fairfax, Virginia 22030

(Dated: September 20, 2021)

We present a scalable set of universal gates and multiply controlled gates in a qudit basis through a bijective mapping from  $N$  qubits to qudits with  $D = 2^N$  levels via rotations in  $U(2)$ . For each of the universal gates ( $H$ ,  $CNOT$ , and  $T$ ), as well as the  $NOT$  gate and multiply-controlled- $Z$  gates, we describe a systematic approach to identifying the set of  $U(2)$  rotations required to implement each gate for any qudit of size  $D$  and with minimal use of an ancilla level. The qudit gates are analyzed in terms of the total rotation count and gate depth as the system scales with  $D$ . We apply the qudit-basis gates to Grover's Algorithm and compare the circuit depth vs. system size to a qubit-based circuit. The results show that there is a dramatic reduction in circuit depth as the size of the system increases for the qudit circuit compared to qubit circuit. In particular, multiply controlled gates are the driving factor in the reduction of circuit complexity for qudit-based circuits since the gate depth remains constant as the system scales with  $D$ .

## I. INTRODUCTION

The development of quantum algorithms and implementation has been focused on qubit-based systems [1-5]. A quantum algorithm is implemented on quantum processors through a quantum circuit constructed with a set of universal gates, such as, the commonly used Hadamard ( $H$ ),  $\pi/8$ -phase ( $T$ ), and controlled-not ( $CNOT$ ) gates. The success of the qubit-based circuit model of quantum computation is rooted in its universality realized through "local" gates operating on single or two qubits [6,7]. On the hardware level, these gates are composed with finite rotation operators (or conditional rotation operators in  $CNOT$  gate) in the 2-dimensional Hilbert space of a qubit driven by external Hamiltonians.

Optimization of quantum circuits have attracted extensive efforts due to its significance in studying theoretical complexity bounds for a given algorithm. It is also critical for implementing an algorithm successfully on hardware available currently or in the near future. For practical reasons, circuit complexity analysis usually includes two parts: the total gate count that can be either the basic universal gates or rotation operators in a circuit, and the circuit depth that counts the number of gates (or rotations) on the longest gate sequence in the circuit. In a noisy intermediate-scale quantum computer, limited coherence time sets an upper bound for the circuit depth and errors in quantum gates accumulates with the total number of gates. [8] In addition, two-qubit gates, such as  $CNOT$  and controlled- $Z$  ( $CZ$ ) gates, are currently the dominant

sources of error due to their higher error rates compared with single qubit gates.

Multiple-qubit gates, such as Toffoli and doubly-controlled- $Z$  gates and their multiply-controlled versions, need complex circuits to implement in a qubit-based system. A Toffoli gate with  $N - 1$  controls and one target qubit can be implemented with an  $N$ -qubit circuit of quadratic depth and gate count  $\mathcal{O}(N^2)$ [9]. The complexity can be reduced to  $\mathcal{O}(N)$  with the help of at least one ancillary qubit [9-11]. It has also been proven that such a qubit-based circuit needs at least  $2N$   $CNOT$  gates [12]. The theoretical lower bound of the circuit depth is still unknown. However, the existing schemes with the least depth of  $\mathcal{O}(\log N)$  requires extra resources including  $\mathcal{O}(N)$  clean ancillary qubits and disentangling operations conditional on measurement results [11].

A quantum computer using one or more qudits rather than an all-qubit system may provide a viable solution in reducing circuit complexity, especially when involving multiple-qubit gates as mention above [13-17].

In this paper, we will focus on methods for mapping qubit-specified gates for an arbitrary  $N$ -qubit system to one qudit of dimension  $D = 2^N + 1$ , where the extra level is needed in some cases. The universal gate set, as well as some important multiply-controlled gates and combinations of multiple single qubit gates applied in parallel will be considered. We assume the computational resources available are rotations in 2-dimensional subspaces of the qudit with fixed angles in integer number of  $\pi/2$ . Circuit complexity is analyzed in term of the rotation operators. Our results show

---

<sup>1</sup> [prambow@gmu.edu](mailto:prambow@gmu.edu)

<sup>2</sup> [mtian@gmu.edu](mailto:mtian@gmu.edu)

significant reduction in both total rotation count and circuit depth in the  $(N - 1)$ -controlled-Z gate that can be constructed with a single  $2\pi$  rotation independent of  $N$ . Circuit depth for a single qubit gate remains constant while the total rotation count increases in  $\mathcal{O}(D)$ . Furthermore, the complexity remains the same when a single qubit gate, such as  $T$  or  $NOT$  gate is applied to multiple qubits in parallel. The most complex gate is the  $H$  gate. When applied to multiple qubits, the rotation count grows in  $\mathcal{O}(DN)$  and depth, in  $\mathcal{O}(N)$ . We will apply these features to show the reduction of circuit complexity, both in overall rotation counts and the circuit depth in Grover's algorithm implemented in a qudit.

The rest of the paper is arranged in three main sections. In Sec. IIA we first lay the framework to express qudit gates in a qubit basis along with the generalized construction of qudit gates via unitary rotations in the  $U(2)$  subspaces. Next in Sec IIB, we describe the specific sequence of rotations to construct the universal gate set, some commonly used gate combinations, as well multiply-controlled-Z gates. In Sec. III we implement Grover's algorithm using qudit gates and analyze the complexity of the circuits in a qudit vs. qubit systems. In Sec. VI we summarize our results and discuss prospective work.

## II. QUANTUM GATES

### A. Qubit-specified gates in qudit basis

The state vector for an arbitrary qudit of dimension  $D$  is a linear superposition of the orthonormal basis of the qudit,  $\{|d\rangle_D\}_{d \in \{0 \dots D-1\}}$ ,

$$|\phi\rangle = \sum_{d=0}^{D-1} \alpha_d |d\rangle_D,$$

where  $\alpha_d$  denotes a set of complex probability amplitudes. The subscript  $D$  outside the basis ket indicates the total size of the system. For simplicity, we will restrict to  $D = 2^N$  that is equivalent to a system of  $N$  qubits. The basis vector mapping between a  $D$ -dimensional qudit and  $N$  qubits is the tensor product of the individual qubit basis,

$$|d\rangle_D = |q_1 q_2 \dots q_i \dots q_N\rangle, \quad (1)$$

where the  $i \in \{1, 2, \dots, N\}$  and  $q_i \in \{0, 1\}$ . The transformation between the two sets of bases is connected through the integer  $d$  and its matching Boolean bit string  $q_1 q_2 \dots q_i \dots q_N$ .

This provides a direct one-to-one mapping between qudit and qubit states. However, the characteristics of a

state may be explicitly shown in the qubit representation, but not in the qudit. For a  $D = 8$  qudit, the superposition between  $|0\rangle_8$  and  $|4\rangle_8$  is an example of a separable qubit state,

$$\frac{1}{\sqrt{2}}(|0\rangle_8 + |4\rangle_8) = \frac{1}{\sqrt{2}}(|0\rangle + |1\rangle) \otimes |00\rangle.$$

A qudit state with a similar structure consisted of  $|0\rangle_8$  and  $|7\rangle_8$  represents a maximally entangled qubit GHZ state,

$$|GHZ\rangle = \frac{1}{\sqrt{2}}(|0\rangle_8 + |7\rangle_8) = \frac{1}{\sqrt{2}}(|000\rangle + |111\rangle).$$

In the qudit basis, both states appear similar and may be prepared by similar operations while in the qubit basis the separable state is prepared by single qubits gates and the GHZ states need qubit-entangling gates.

In this section we will present the construction of universal gates, as well as some commonly used gate combinations in the qudit basis through rotation operators in 2-dimensional subspaces. The qudit construction of equivalent one- and two-qubit gates are generally "single action" gates. The action of the qudit operator in effect equivalently transforms a single target qubit  $t$ ,

$$U^t |d\rangle_D = U^t |q_1 \dots q_t \dots q_N\rangle = |q_1 \dots q'_t \dots q_N\rangle.$$

For a two-qubit controlled gate the nomenclature is  $U^{c,t}$ , where  $c$  and  $t$  denote the control and target qubits, respectively.

Any operator acting on the  $D$ -dimensional Hilbert space transforms a qudit state and the equivalent multiple-qubit states in the same manner due to the bijective mapping between the bases. However, the implementation of qubit-based universal gates cannot be directly applied to a qudit. An operator addressing a single or the two qubits can be realized "locally" in the corresponding one- or two-qubit subspace while the same operator on a qudit may involve operations in the entire Hilbert space.

The qubit-based gates are implemented by  $U(2)$  rotations in a 2-dimensional space spanned by the qubit basis. The finite rotation operator for such a two-state system is,

$$R_{\hat{n}}(\theta) = \exp\left(\frac{-i\theta(\boldsymbol{\sigma} \cdot \hat{\mathbf{n}})}{2}\right),$$

where  $\boldsymbol{\sigma} \cdot \hat{\mathbf{n}}$  is the Pauli vector. The axis and angle of rotation are denoted by  $\hat{\mathbf{n}}$  and  $\theta$ , respectively.

In order to compose the qudit gates it is assumed that the same rotations are available in the subspaces

spanned by any pair of the qudit basis vectors. The generalized expression for a  $U(2)$  rotation in the subspace of a qudit is given by,

$$R_{\hat{n}}^{(j,k)}(\theta) = \exp\left(\frac{-i\theta(\boldsymbol{\sigma} \cdot \hat{\mathbf{n}})}{2}\right)^{(j,k)} \oplus \mathbb{I}_{D-1}^{(j,k)}, \quad (2)$$

where  $j < k \in \{0,1,2, \dots, D\}$  are the qudit levels under rotation. The first  $D$  levels are the qudit basis vectors in Equation (1) and the  $D$ th is an ancillary level necessary for some of the gates.

Use of the rotations in subspaces comes with a caveat in the form of a local phase. Since the operator in a higher dimension as shown in Equation (2) is a tensor sum of an identity and a rotation operator, a global phase in a  $U(2)$  rotation becomes a local phase in  $U(D)$ . The ancillary level is included to ensure the rotation operators belong to  $SU(2)$  in that a local phase is not imparted to the basis qudit. It should be noted that not all gates require the ancilla level.

Any qudit unitary can be constructed through a sequence of  $U(2)$  rotations of selected axes, rotation angles, and pairings of qudit levels. The complexity analysis of a gate construction includes the number of the rotations and the depth of the circuit in terms of rotation count on the longest sequence. Our goal is to reduce the rotation count and the circuit depth. Commutation properties among the rotation operators helps to achieve reduction in both. Two useful commuting rotations are

1. Rotations operating on entirely different qudit levels commute,

$$\left[R_{\hat{n}'}^{(j,k)}(\theta'), R_{\hat{n}}^{(l,m)}(\theta)\right] = 0.$$

2. Two rotations which share a common level commute if they share a set of eigenvectors in the Hilbert space spanned by all levels involved,

$$\left[R_{\hat{n}'}^{(j,k)}(\theta'), R_{\hat{n}}^{(j,m)}(\theta)\right] = 0.$$

One example is the operators whose eigenvectors are the qudit basis. These operators include all rotations by  $2\pi (-I)$  and all rotations about z-axis.

In the following sections we present constructions of the three universal gates ( $H$ ,  $CNOT$ , and  $T$ ), as well as  $NOT$  and multiply-controlled- $Z$  gates, for a qudit system of dimension  $D = 2^N$  using the qudit rotation operator (Equation 2). We will show it is sufficient to set the axes of rotations to x, y, and z, and limit rotation angles to  $\pm n\pi/2$  for integer  $n$ .

## B. Universal Gate Set

### Hadamard Gate

The single-action qudit Hadamard gate,  $H^{t=i}$ , applied on a qudit basis creates a superposition between two qudit levels that is equivalent to a Hadamard gate applied to the  $t$ -th qubit,

$$\begin{aligned} H^t |d\rangle_D &= H^t |q_1 q_2 \dots q_t \dots q_N\rangle \\ &= |q_1 q_2 \dots\rangle \otimes H |q_t\rangle \otimes |\dots q_N\rangle. \end{aligned}$$

The  $D$  basis vectors of a qudit are paired into  $D/2$  pairs identified by a lower and upper indices,  $l$  and  $u$ ,

$$|l\rangle_D = |q_1 q_2 \dots q_t = 0 \dots q_N\rangle$$

$$|u\rangle_D = |q_1 q_2 \dots q_t = 1 \dots q_N\rangle.$$

The operator  $H^t$  should transform every pair in the same way,

$$\begin{aligned} H^t |l\rangle_D &= \frac{1}{\sqrt{2}} (|l\rangle_D + |u\rangle_D) \\ H^t |u\rangle_D &= \frac{1}{\sqrt{2}} (|l\rangle_D - |u\rangle_D). \end{aligned}$$

A  $y$ -rotation  $R_y(-\pi/2)$  in the subspace spanned by a pair of  $|l\rangle_D$  and  $|u\rangle_D$  creates a superposition of the two with a wrong sign for the upper level  $|u\rangle_D$ . Subsequently, all upper levels can be paired up to form a new set of subspaces where a  $x$ -rotation  $R_x(2\pi)$  corrects the sign of the upper basis vectors. The correction is required for the upper states of the  $y$ -rotations which are addressed an odd number of times.

Table I. shows an example of a qudit Hadamard gate on a qudit of dimension  $D = 8$  on which a single  $H$  gate is applied to the first qubit. The lower index  $l = 0, 1, 2,$  and  $3$  pairs with the upper index  $u = 4, 5, 6,$  and  $7$ , respectively. The  $y$ -rotations create the superposition within a pair, such as,

$$\begin{aligned} R_y^{(0,4)}(-\pi/2): \{|0\rangle_8, |4\rangle_8\} \\ \rightarrow \left\{ \frac{1}{\sqrt{2}} (|0\rangle_8 - |4\rangle_8), \frac{1}{\sqrt{2}} (|0\rangle_8 + |4\rangle_8) \right\} \end{aligned}$$

$$\begin{aligned} R_y^{(2,6)}(-\pi/2): \{|2\rangle_8, |6\rangle_8\} \\ \rightarrow \left\{ \frac{1}{\sqrt{2}} (|2\rangle_8 - |6\rangle_8), \frac{1}{\sqrt{2}} (|2\rangle_8 + |6\rangle_8) \right\}. \end{aligned}$$

The  $R_x(2\pi)$  rotations are applied to all the upper states to correct the sign,  $R_x^{(4,6)}(2\pi): \{|4\rangle_8, |6\rangle_8\} \rightarrow \{-|4\rangle_8, -|6\rangle_8\}$ . All options of one-to-one pairing among the upper levels for the  $x$ -rotations are equivalent. All rotations enclosed in a set of curly brackets in Table I operate in parallel.

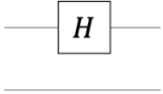
 Equivalent Qubit Hadamard Gate	$H^{t=1} d\rangle_8 = \frac{1}{\sqrt{2}}( 0\rangle \pm  1\rangle) \otimes  q_2 q_3\rangle$
	$H^{t=1} 0\rangle_8 = \frac{1}{\sqrt{2}}( 0\rangle_8 +  4\rangle_8)$ $H^{t=1} 1\rangle_8 = \frac{1}{\sqrt{2}}( 1\rangle_8 +  5\rangle_8)$ $H^{t=1} 2\rangle_8 = \frac{1}{\sqrt{2}}( 2\rangle_8 +  6\rangle_8)$ $H^{t=1} 3\rangle_8 = \frac{1}{\sqrt{2}}( 3\rangle_8 +  7\rangle_8)$ $H^{t=1} 4\rangle_8 = \frac{1}{\sqrt{2}}( 0\rangle_8 -  4\rangle_8)$ $H^{t=1} 5\rangle_8 = \frac{1}{\sqrt{2}}( 1\rangle_8 -  5\rangle_8)$ $H^{t=1} 6\rangle_8 = \frac{1}{\sqrt{2}}( 2\rangle_8 -  6\rangle_8)$ $H^{t=1} 7\rangle_8 = \frac{1}{\sqrt{2}}( 3\rangle_8 -  7\rangle_8)$
$H^{t=1} = \left\{ R_x^{(4,6)}(2\pi) R_x^{(5,7)}(2\pi) \right\}$ $* \left\{ R_y^{(0,4)}\left(\frac{-\pi}{2}\right) R_y^{(1,5)}\left(\frac{-\pi}{2}\right) R_y^{(2,6)}\left(\frac{-\pi}{2}\right) R_y^{(3,7)}\left(\frac{-\pi}{2}\right) \right\}$	

Table I. Qudit Hadamard gate example for a  $D = 8$  system with the  $H$  gate action on the  $t = 1$  equivalent qubit. The operator reads from right to left.

The total rotation count for a single-action qudit Hadamard gate is  $3D/4$ . All  $R_y(-\pi/2)$  rotations can be run in parallel, as well as all  $R_x(2\pi)$ . Therefore, the circuit depth is 2, independent of the system size. There are  $N$  single-action  $H$  gates for a  $D = 2^N$  qudit system and each can be implemented in the same manner with different qudit level pairings.

It is quite common in an algorithm that a set of qubit  $H$  gates are applied to a few or all qubits in parallel. Any combination of parallel single-action  $H$  gates can be expressed as a qudit  $H$  gate made by a sequence of y- and x-rotations Figure 1. shows the rotation sequence implementing  $H$  gates to all three qubits in a  $D = 8$  qudit. The level pairings for the corresponding rotations are indicated by the double-sided arrows. In this depiction, the rotations are performed from left to right as in a circuit. The three sets of  $R_y(-\pi/2)$  rotations create a uniform superposition between all eight levels up to a sign. For a  $D = 2^N$  qudit, there are  $N$  sets of y-rotations and  $D/2$  rotations operating in parallel in each set. The span between the paired levels of the  $i$ th set is given by  $2^{N-i}$ , where  $i \in \{1, \dots, N\}$ . Just as with the single-action  $H$  gate, the levels for the  $R_x(2\pi)$  rotations are found by identifying the set of upper-states from the  $R_y(-\pi/2)$  rotations which are addressed an odd number of times. There are  $D/4$  pairings for the  $R_x(2\pi)$  rotations.

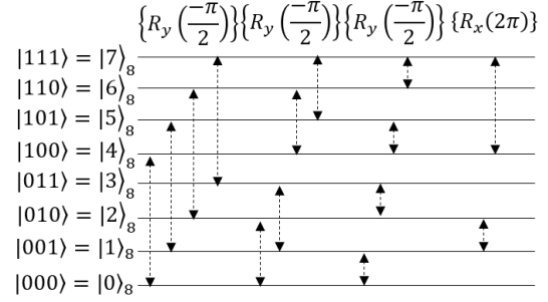


Figure 1. An  $H$  gate with action on all equivalent qubits for a  $D = 8$  qudit system requires a total of 14 rotations. The dashed arrows indicated the levels addressed by each rotation. Each set of rotations in curly brackets commute and can be performed in parallel. For this Hadamard gate, the circuit gate depth grows with system size as a function of  $N + 1$ . The operator sequence read from left to right.

For the multi-action qudit  $H$  gate (equivalent to  $N$  qubit  $H$  gates in parallel) the total rotation count is  $D(2N + 1)/4$ . All  $R_y(-\pi/2)$  rotations within a set can be run in parallel, as well as all  $R_x(2\pi)$ . Therefore, the circuit depth scales with the system size as  $N + 1$ .

For an arbitrary number of  $M$  qubit Hadamard gates applied in parallel, where  $1 \leq M \leq N$ , the rotation sequence is simply a subset of the  $N$  sets of y-rotations for the multi-action Hadamard gate. The subset of y-rotations for a qudit  $H$  gate corresponds to the subset of qubits in an equivalent qubit circuit transformed by the  $H$  gates in parallel. For example, in a  $D = 8$  system the  $H$  gate,  $H^{t=1,3}$ , has two sets of y-rotations where  $t \in \{1,3\}$  with the spacing of the level pairings for each subset given by  $2^{N-t}$ . The correction for -1 phase of the upper states is performed by a set of x rotations selected and paired in the same manner as described above.

For the  $M$ -action qudit  $H$  gate the total rotation count is  $D(2M + 1)/4$ . All  $R_y(-\pi/2)$  rotations within a set can be run in parallel, as well as all  $R_x(2\pi)$ . Therefore, the circuit depth scales with the number of targets as  $M + 1$  with the circuit depth upper limit when  $M = N$ .

### CNOT Gate

The qudit  $CNOT$  gate performs the same action as an equivalent qubit  $CNOT$  gate where the target state is flipped predicated on the state of the control qubit,

$$C_x^{c,t}|d\rangle_D = C_x^{c,t}|q_1 \dots q_c \dots q_t \dots q_N\rangle = |q_1 \dots q \dots (q_c \oplus q_t) \dots q_N\rangle.$$

This gate can be implemented with a set of rotations in  $U(2)$  subspaces,

$$C_x^{c,t} = \prod \{R_y^{a,b}(\pi)\} \{R_x^{b,c}(2\pi)\},$$

where the indices  $a, b$ , and  $c$  are chosen according to a given pair of control and target.

The scheme is also explained in an example described in Table II. with a set of rotations for a qubit  $CNOT$  gate,  $C_x^{1,2}$ , in a  $D = 16$  qudit system. A  $R_y(\pi)$  rotation pairs two qudit levels where the control and target qubits are in  $|10\rangle$  and  $|11\rangle$  while the remaining of qubits are in identical separable states. There are  $D/4$  such pairs as listed in the table. These rotations flip the paired levels and impart a “-“ to the  $|11\rangle$  states for the control and target qubits. For example,  $R_y^{(9,13)}(\pi): \{|9\rangle_{16}, |13\rangle_{16}\} \rightarrow \{-|13\rangle_{16}, |9\rangle_{16}\}$ . The local phase is reset by an  $x$ -rotation, such as  $R_x^{(13,12)}(2\pi)$ , which resets the local phase in another pair  $\{|12\rangle_{16}, |8\rangle_{16}\}$  simultaneously. There are  $D/8$   $R_x(2\pi)$  rotations for  $D \geq 8$ . For  $D = 4$ , where the local phase is present in only one level an ancillary level is needed to compensate the local phase.

The total rotations count is  $3D/8$ . All  $R_y(\pi)$  rotations can be run in parallel, as well as all  $R_x(2\pi)$ . Therefore, the circuit depth is 2, independent of the system size.

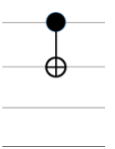
 Equivalent Qubit CNOT Gate	$ d\rangle_{16} =  q_c q_t q_3 q_4\rangle =  q_c q_t\rangle \otimes  q_3 q_4\rangle$
	$ 15\rangle_{16} =  1111\rangle =  11\rangle \otimes  11\rangle$ $ 11\rangle_{16} =  1011\rangle =  10\rangle \otimes  11\rangle$
	$ 14\rangle_{16} =  1110\rangle =  11\rangle \otimes  10\rangle$ $ 10\rangle_{16} =  1010\rangle =  10\rangle \otimes  10\rangle$
	$ 13\rangle_{16} =  1101\rangle =  11\rangle \otimes  01\rangle$ $ 9\rangle_{16} =  1001\rangle =  10\rangle \otimes  01\rangle$
	$ 12\rangle_{16} =  1100\rangle =  11\rangle \otimes  00\rangle$ $ 8\rangle_{16} =  1000\rangle =  10\rangle \otimes  00\rangle$
$C_x^{1,2} = \{R_y^{(11,15)}(\pi)R_y^{(10,14)}(\pi)R_y^{(9,13)}(\pi)R_y^{(8,12)}(\pi)\} * \{R_x^{(15,14)}(2\pi)R_x^{(13,12)}(2\pi)\}$	

Table II.  $CNOT$  gate example of the paired levels for the  $\pi$  rotation about the  $y$ -axis for a qudit of dimension  $D = 16$ . For each level pairing the control qubit is 1, the target qubit is either 0 or 1, and the remaining qubits are in an identical separable state.

A multiple control qudit  $CNOT$  gate rotation sequence can be construction based on the same principles, i.e. the level pairing for  $R_y(\pi)$  is between the states where the target qubit in  $|1\rangle$  and  $|0\rangle$  and all control qubits in  $|1\rangle$  and the remaining no-action qubits in an identical qubit basis state. The number of pairs is the number of orthogonal basis of the non-action qubits. For  $C$  control qubits and 1 target in a  $D = 2^N$  qudit, there are  $2^{N-C-1}$  pairs, which is also the number of  $R_y(\pi)$  rotations. In a system with at least one non-action qubit, the local phase in each pair can be compensated by a  $R_x(2\pi)$  between two pairs as discussed above. The total operator count is

$3(2^{N-C-1})/2$  for  $N - C \geq 2$ . In the cases where all qubits are involved, i.e.  $C = N - 1$ , the multiple  $CNOT$  can be implemented with one  $R_y(\pi)$  and followed by a  $R_x(2\pi)$  to an ancillary level.

The trend that the required operators decrease with the number of controls in a  $CNOT$  gate is the opposite to the traditional implementation in a qubit system. Furthermore,  $CNOT$  with multiple controls constructed in a qudit system has a constant depth of 2, independent of the size of the system and number of controls.

### T Gate

The  $T$  gate imparts a phase of  $exp(i\pi/4)$  to the qudit levels corresponding to the target qubit in  $|1\rangle$ ,

$$T^t|d\rangle_D = T^t|q_1 \dots q_t \dots q_N\rangle = exp(i\pi q_t/4)|q_1 \dots q_t \dots q_N\rangle.$$

There are  $D/2$  levels, each requires one rotation about the  $z$ -axis by  $-\pi/2$  to the ancillary level. The generalized rotations sequence is,

$$T = \prod \left\{ R_z^{(a,D)} \left( \frac{-\pi}{2} \right) \right\},$$

where index  $a$  includes  $D/2$  levels of  $q_t = 1$ . Table III shows an example of a  $T$  gate applied to the  $t = 2$  equivalent qubit.

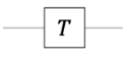
 Equivalent Qubit $\pi/8$ Phase Gate	$T^{t=2} d\rangle_8 = T^{t=2} q_1 q_2 q_3\rangle$
	$T^{t=2} 0\rangle_8 = T^{t=2} 000\rangle =  0\rangle_8$ $T^{t=2} 1\rangle_8 = T^{t=2} 001\rangle =  1\rangle_8$ $T^{t=2} 2\rangle_8 = T^{t=2} 010\rangle = e^{i\pi/4} 2\rangle_8$ $T^{t=2} 3\rangle_8 = T^{t=2} 011\rangle = e^{i\pi/4} 3\rangle_8$ $T^{t=2} 4\rangle_8 = T^{t=2} 100\rangle =  4\rangle_8$ $T^{t=2} 5\rangle_8 = T^{t=2} 101\rangle =  5\rangle_8$ $T^{t=2} 6\rangle_8 = T^{t=2} 110\rangle = e^{i\pi/4} 6\rangle_8$ $T^{t=2} 7\rangle_8 = T^{t=2} 111\rangle = e^{i\pi/4} 7\rangle_8$
$T^{t=2} = \left\{ R_z^{(2,8)} \left( \frac{-\pi}{2} \right) R_z^{(3,8)} \left( \frac{-\pi}{2} \right) R_z^{(6,8)} \left( \frac{-\pi}{2} \right) R_z^{(7,8)} \left( \frac{-\pi}{2} \right) \right\}$	

Table III.  $T$  gate example in a qudit of size  $D = 8$  where the qubit equivalent  $T$  gate is applied to the second qubit in the circuit.

The depth of the  $T$  gate is a constant 1 since all  $R_z(-\pi/2)$  rotations commute and can be executed in parallel. This gate can be constructed with the same number of  $R_z(-\pi/4)$  rotations without ancillary level.

### C. Additional Gates

In a similar manner presented in the previous section, any single-qubit and two-qubit gate can be implemented in a qudit system with rotations in  $U(2)$  subspaces. In most of the cases, a set of rotations are needed to compensate unintended local phases,

sometimes via an ancillary level. Implementation of multiple gates on different qubits and multiply-controlled gates may be significantly simplified in a qudit. An example in each case will be given in this section.

#### NOT Gate

A single qubit NOT gate is a Pauli-X operator that flips the target qubit state between  $|0\rangle$  and  $|1\rangle$ ,

$$X^t |d\rangle_D = |q_1 q_2 \dots\rangle \otimes X |q_t\rangle \otimes |\dots q_N\rangle.$$

In a qudit, the state pairing is similar to the *CNOT* gate. A pair consists of two levels where the target qubit state in  $|0\rangle$  and  $|1\rangle$  and the remaining qubits in an identical basis. There are  $D/2$  pairs in the system, which requires  $D/2$   $R_y(\pi)$  and  $D/4$   $R_x(2\pi)$  rotations. All  $R_y(\pi)$  rotations can be run in parallel, as well as all  $R_x(2\pi)$ . To complete a  $X$  gate, the same as in the *CNOT* gate, the circuit depth is a constant 2.

For  $D = 8$ , a single  $X$  gate requires 6 rotations. Two  $X$  gates each addressing a different qubit are also constructed with 6 rotations. Identifying the rotation level pairing for any combination of  $X$  gates in parallel, such as shown in Table IV, is a simple matter of determining the bijective mapping of a set of qudit basis to itself. A mapping example is in Table IV, where  $X$  gates are applied to the 1<sup>st</sup> and 2<sup>nd</sup> qubits. Due to the bijective mapping, the total numbers of  $R_y(\pi)$  and  $R_x(2\pi)$  rotations for  $X$  gates remains  $D/2$  and  $D/4$ , respectively, independent of the number of  $X$  gates.

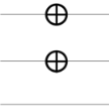
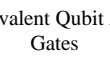
	$X^{1,2}  d\rangle_8 = X^1 X^2  q_1 q_2 q_3\rangle$
	$X^{1,2}  0\rangle_8 =  110\rangle =  6\rangle_8$ $X^{1,2}  1\rangle_8 =  111\rangle =  7\rangle_8$ $X^{1,2}  2\rangle_8 =  100\rangle =  4\rangle_8$ $X^{1,2}  3\rangle_8 =  101\rangle =  5\rangle_8$ $X^{1,2}  4\rangle_8 =  010\rangle =  2\rangle_8$ $X^{1,2}  5\rangle_8 =  011\rangle =  3\rangle_8$ $X^{1,2}  6\rangle_8 =  000\rangle =  0\rangle_8$ $X^{1,2}  7\rangle_8 =  001\rangle =  1\rangle_8$
Equivalent Qubit NOT Gates	
$X^{1,2} = \{R_y^{(0,6)}(\pi)R_y^{(1,7)}(\pi)R_y^{(2,4)}(\pi)R_y^{(3,5)}(\pi)\} * \{R_x^{(6,8)}(2\pi)R_x^{(7,8)}(2\pi)R_x^{(4,8)}(2\pi)R_x^{(5,8)}(2\pi)\}$	

Table IV.  $X$  gate example of the paired levels for a qudit system of size  $D = 8$ . The level pairings for the y-axis rotations are between the qudit input/output states, while the x-axis rotations correct for the phase for the upper-level states.

#### Multiply-Controlled-Z Gate

The qudit multiply-controlled-Z gate imparts a phase of  $\exp(i\pi) = -1$  to the states where, in the qubit basis, the target qubit and the control qubits are  $|1\rangle$ . In a  $D = 2^N$  dimensional qudit with  $N - 1$  control qubits and one target, a controlled-Z gate imparts a “-“ sign on a single level,

$$|1\rangle^{\otimes D} = |D - 1\rangle \rightarrow -|1\rangle^{\otimes D} = -|D - 1\rangle.$$

This is the same transformation for any combination of the control and target assignment. A single rotation of  $2\pi$  about the z-axis between this level and the ancillary is all that is required to construct a qudit multiply-controlled-Z gate,

$$C_Z^{D-1} = R_Z^{(D-1,D)}(2\pi).$$

In fact, the rotation axis can be in any direction in the  $U(2)$  subspace spanned by the qudit basis vectors  $|D - 1\rangle_D$  and  $|D\rangle_D$ . A multiply-controlled-Z gate is the core operation in many quantum algorithms, such as Grover’s research algorithm. Implementing it in a qudit basis can simplify a quantum circuit significantly over the conventional qubit basis operation.

Where the total number of action qubits is less than the size of the system, there are more than one qudit levels affected by the controlled-Z gates, which are the levels correspond to all action qubits in  $|1\rangle$ . There are  $2^{N-C-T}$  such levels for  $C$  control qubits and  $T$  target qubits. The phase can be implemented by  $2\pi$  rotations between any pair of these levels, that is a total  $2^{N-C-T-1}$  rotations. Table V shows an example of a  $Z$  gate controlled by two qubits in a qudit system of size  $D = 16$ .

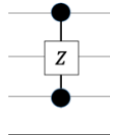
	$ q_c q_t q_c q_t\rangle$
Equivalent Qubit Multiply-Controlled-Z Gate	$ 15\rangle_{16} =  1111\rangle$ $ 14\rangle_{16} =  1110\rangle$
$C_z^{c,t} = R_z^{(15,14)}(2\pi)$	

Table V. The rotations to construct a qudit multiply controlled-Z gate, equivalent to the qubit gate diagram shown, requires two rotations by  $2\pi$  about the z-axis. The rotation levels are between the ancilla and the states where the controlled and target inputs are 1. For a  $D = 16$  qudit system there are two states which satisfy the conditions.

The depth of the qudit multiply-controlled  $Z$  gate is 1, regardless of the size of the system, or the number of rotations to construct the qudit gate. This is because all rotations commute.

### III. GROVER’S ALGORITHM

In this section we analyze the circuit complexity of the Grover’s Algorithm with a qudit and compare the circuit depth, as a function of equivalent system size for



a qubit-based circuit [9,18-20]. Whether using qubits or qudits, Grover's algorithm is implemented through the same sequence of circuit modules presented by the blocks in Figure 2 [21,22].

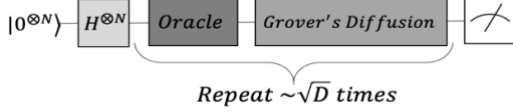


Figure 2. Grover's algorithm functional diagram for qubits and qudits.  $H^{\otimes N}(2|0\rangle\langle 0| - I_D)H^{\otimes N}$  is the Grover's Diffusion operator. [18]

The first step is to initiate the qudit (or qubits) from the ground state into a superposition of all basis vectors using a Hadamard gate. For a qubit system, the Hadamard gate, which has a depth of 2, is applied in parallel to each qubit in the circuit. For a qudit system, a single multi-action Hadamard gate is applied to the qudit. Recall the qudit multi-action Hadamard gate depth grows linearly as  $N + 1$ .

In the superposition, each basis vectors represent an entry in the search list of size  $D$  with one desired entry in the list to be "marked" by the oracle. The oracle module flips the sign of the probability amplitude for the term representing the marked entry while leaving the rest of system unchanged. In the construction of this module, the simplest case for the oracle is the  $(N - 1)$ -controlled-Z gate which specifies the state  $|D - 1\rangle = |1\rangle^{\otimes N}$  as the marked entry. In a more general case, where the oracle function marks any other bit string, the  $(N - 1)$ -controlled-Z gate should be executed in condition of the control qubits in the basis state matching the bit string. This can be implemented with an additional set of parallel NOT gates before and after the regular  $(N - 1)$ -controlled-Z gate.

For the qudit system, an oracle with a  $(N - 1)$ -controlled-Z gate has a constant circuit depth of 1. In the conventional qubits basis, implementation of the oracle with an  $(N - 1)$ -controlled-Z gate requires a circuit depth growing quadratically with the system size  $N$  [9]. It has been proposed that the qubit circuit can be reduced to a linear depth growth of  $8N - 20$  [23]. The addition of two sets of parallel NOT gates to the oracle would add a constant depth of 2 for a qubit system, and a constant depth of 4 for a qudit system.

The output from the oracle module, is fed to Grover's Diffusion module with operational block diagram shown in figure 3. The diffusion operator increases the probability amplitude for the marked term by flipping the probability amplitudes of all terms in the superposition about the average. In a qudit system the diffusion operator grows linearly as  $2N + 7$ , with the two multi-action Hadamard gates the driver in the linear

term since the X gates and  $(N - 1)$ -controlled-Z gate are constant in depth (2 and 1 respectively). Operating in the qubit basis, the H and X gates have constant depths (2 and 1 respectively), but the module has a quadratic circuit depth due to the  $(N - 1)$ -controlled-Z gate [9]. The diffusion module depth can be reduced to a linear depth of  $8N - 14$ , employing the same technique for the  $(N - 1)$ -controlled-Z gate as in the oracle[23].

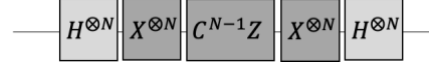


Figure 3. Generalized circuit implementation of Grover's Diffusion operator. For qudits of dimension  $2^N$ , Hadamard gates are applied in series and the set has a depth of  $N+1$ . The qudit NOT gates have a depth of 2 and the  $(N-1)$ -controlled-Z gate has a depth of 1.

In order to increase the probability of measuring the marked term, Grover's Algorithm runs the superposition through the oracle and diffusion modules  $t$  times, where  $t \propto O(\sqrt{D})$ . As a result, the combined circuit depth for the oracle and diffusion modules contribute a multiple of  $t$  times to the total circuit depth required to run Grover's algorithm to maximum theoretical accuracy.

Finally, we compare the total circuit depth results for  $t$  iterations of Grover's algorithm for increasing qudit and qubit system size. The decomposition of the multiply-controlled-Z gate into elementary gates results in a quadratic growth in depth for the qubit system. With the multiply-controlled-Z gate appearing in both the oracle and the diffusion operator the total depth of the qubit circuit is dominated by this quadratic growth. Clearly, the circuit depth of a qubit system with quadratic growth will grow faster than a linear based qudit or qubit system. Instead, we compare the two systems with linear circuit depth growth.

The total circuit depth for Grover's algorithm, with  $(N - 1)$ -controlled-Z gate as the oracle, using a qudit system grows linearly as  $t(2N + 8) + N + 1$  for a given number of  $t$  iterations. For a qubit system, with a linear construction of the  $(N - 1)$ -controlled-Z gate, the overall circuit depth for  $t$  iterations grows as  $t(16N - 34) + 2$ . Table VI shows the total circuit depth for maximum theoretical accuracy of Grover's algorithm for a qudit system and a qubit system, where the gates are implemented by pulses ( $U(2)$  rotations). As the system size increases, the circuit depth to run Grover's algorithm with high theoretical accuracy, qudit gates show a significant reduction in circuit depth compared to qubit gates.

Equivalent N qubits (D = levels)	Iterations (t)	Theoretical Accuracy	Grover's Algorithm Total Depth (Pulses in Parallel)	
			Qudit	Qubits
3 (D = 8)	2	97.23%	32	30
4 (D = 16)	3	98.05%	53	92
5 (D = 25)	4	99.96%	78	186
6 (D = 36)	6	99.83%	127	374
7 (D = 49)	8	99.78%	184	626

Table VI. Grover's Algorithm theoretical accuracy and total circuit depth for qubits and qudit gates implemented using pulses. Entries in white are the smallest number of iterations for first maximum in accuracy.

#### IV. SUMMARY

We have presented a systematic and scalable construction of qudit-based quantum gates through a bijective mapping between the computation basis of  $N$  qubits and the  $D = 2^N$  levels in a qudit of size  $D + 1$ . The composition complexity of the qudit-based gates has been analyzed in terms of the total number of basic  $U(2)$  rotations and the circuit depth. For the universal qubit gate set ( $H$ ,  $CNOT$ , and  $T$ ) implemented with a qudit the total number of rotations is linear to  $D$  ( $3D/4$ ,  $3D/8$ , and  $3D/4$ , respectively) while the circuit depth remains constant (2, 2, and 1, respectively) regardless of the system size. In general, a single qubit gate requires rotations in multiple orthogonal subspaces in a qudit. The number of the subspaces specified by the qudit level pairing grows linearly with  $D$  while the rotations in all orthogonal subspaces can be executed in parallel. In a qubit circuit, a single qubit gate can be applied to some or all qubits in parallel, while the complexity of the corresponding implementation in a qudit depends on the gate. The multiple qubit gate  $H^{\otimes M}$  requires  $D(2M + 1)/4$  rotations with circuit depth  $M + 1$ . The complexity for  $X^{\otimes M}$  stays the same as a single  $X$  gate. Qudit implementation greatly favors multiply-controlled gates, such as controlled- $NOT$  and controlled- $Z$ . The depth remains constant (2 for controlled- $NOT$  and 1 for controlled- $Z$ ) independent of the system size. The required number of rotations decreases exponentially with the number of control qubits down to 2 for controlled- $NOT$  and 1 for controlled- $Z$  at  $(N - 1)$  control qubits.

Compared with qubit-based circuits, a qudit implementation is advantageous where the multiply controlled gates are employed. A significant circuit depth reduction has been shown in Grover's Algorithm. Using either the standard set of qubit elementary gates, or optimizing the circuit using linear depth multiply controlled- $Z$  gates, the depth of Grover's Algorithm grows quickly as the system size increases. Comparatively, the depth of Grover's Algorithm using qudits grows slowly as the system size increases, giving qudit circuits an advantage in depth over qubits.

Qudit basis computation may find other applications where multiply controlled gates apply an important role. It will be of interest in future study to analyze the measurement schemes and consequence in single qudit, as well as gates and measurement in qubit-qudit or qudit-qudit systems.

- [1] Arute, F. et al. Quantum supremacy using a programmable superconducting processor. *Nature* **574**, 505–510 (2019).
- [2] Gambetta, J. IBM's Roadmap For Scaling Quantum Technology (2020). URL <https://www.ibm.com/blogs/research/2020/09/ibm-quantumroadmap>.
- [3] Wright, K. et al. Benchmarking an 11-qubit quantum computer. *Nat. Commun.* **10**, 5464 (2019)
- [4] Grzesiak, N., Blümel, R., Wright, K., Beck, K. M., Pienti, N. C., Li, M., ... & Nam, Y. (2020). Efficient arbitrary simultaneously entangling gates on a trapped-ion quantum computer. *Nature communications*, *11*(1), 1-6.
- [5] J. M. Arrazola, et al. "Quantum circuits with many photons on a programmable on a programable nanophotonic chip", *nature* *591*, 54-60 (2021).
- [6] M. Nielsen, I. L. Chuang, Quantum Computation and Quantum Information, Cambridge Univ. Press, 2000.
- [7] C. M. Dawson, M. A. Nielsen, "The Solovay-Kitaev Algorithm", *Quantum Inf. Comput.*, Vol. 6, 81–95 (2006)
- [8] Preskill, J. (2012). Quantum computing and the entanglement frontier. *arXiv preprint arXiv:1203.5813*.
- [9] Barenco, A., Bennett, C. H., Cleve, R., DiVincenzo, D. P., Margolus, N., Shor, P., ... & Weinfurter, H. (1995). Elementary gates for quantum computation. *Physical review A*, *52*(5), 3457.
- [10] Maslov, D., Dueck, G. W., & Miller, D. M. (2007). Techniques for the synthesis of reversible Toffoli networks. *ACM Transactions on Design Automation of Electronic Systems (TODAES)*, *12*(4), 42-es.
- [11] He, Y., Luo, M. X., Zhang, E., Wang, H. K., & Wang, X. F. (2017). Decompositions of n-qubit Toffoli gates with linear circuit complexity. *International Journal of Theoretical Physics*, *56*(7), 2350-2361.
- [12] Vivek V. Shende and Igor L. Markov. 2009. On the CNOT-cost of TOFFOLI gates. *Quantum Info. Comput.* *9*, 5 (May 2009), 461–486.
- [13] Ferraro, E., & De Michielis, M. (2020). On the robustness of the hybrid qubit computational gates through simulated randomized benchmarking protocols. *Scientific Reports*, *10*(1), 1-10.
- [14] Low, P. J., White, B. M., Cox, A. A., Day, M. L., & Senko, C. (2020). Practical trapped-ion protocols for universal qudit-based quantum computing. *Physical Review Research*, *2*(3), 033128.
- [15] Kiktenko, E. O., Nikolaeva, A. S., Xu, P., Shlyapnikov, G. V., & Fedorov, A. K. (2020). Scalable quantum computing with qudits on a graph. *Physical Review A*, *101*(2), 022304.
- [16] Dalla Chiara, M. L., Giuntini, R., Sergioli, G., & Leporini, R. (2018). A many-valued approach to quantum computational logics. *Fuzzy Sets and Systems*, *335*, 94-111.



- [17] Kiktenko, E. O., Fedorov, A. K., Strakhov, A. A., & Man'Ko, V. I. (2015). Single qudit realization of the Deutsch algorithm using superconducting many-level quantum circuits. *Physics Letters A*, 379(22-23), 1409-1413.
- [18] M. Nielsen, I. L. Chuang, *Quantum Computation and Quantum Information*, Cambridge Univ. Press, 2000.
- [19] C.Gidney, "Using quantum gates instead of ancillabits," <http://algassert.com/circuits/2015/06/22/Using-Quantum-Gates-instead-of-Ancilla-Bits.html>, 2015, accessed: 2021-07-16.
- [20] Zhang, K., & Korepin, V. E. (2020). Depth optimization of quantum search algorithms beyond Grover's algorithm. *Physical Review A*, 101(3), 032346.
- [21] Wang, Y., & Krstic, P. S. (2020). Prospect of using Grover's search in the noisy-intermediate-scale quantum-computer era. *Physical Review A*, 102(4), 042609.
- [22] Mandviwalla, A., Ohshiro, K., & Ji, B. (2018, December). Implementing Grover's algorithm on the IBM quantum computers. In *2018 IEEE International Conference on Big Data (Big Data)* (pp. 2531-2537). IEEE.
- [23] Saeedi, M., & Pedram, M. (2013). Linear-depth quantum circuits for n-qubit Toffoli gates with no ancilla. *Physical Review A*, 87(6), 062318.